JOURNAL OF KUFA−PHYSICS
www.uokufa.edu.iq/journals/index.php/jkp | ISSN: 2077−5830

Reentry of Space Debris from Low Earth Orbit by Pulsed Nd:YAG Laser

*[1]H. K. Al-Zaidi [2]M. J. Al-Bermani [1]A.M. Taleb

[1]*Department of Physics, College of Sciences, Baghdad University, Baghdad, Iraq.*
[2] *Department of Computer Techniques Eng., University of Alkafeel, Alnajaf, Iraq*

*Corresponding Author E-mail: hamid_alzaidi@yahoo.com

ARTICLE INF

Article history:
Received: 04 APR, 2020
Revised: 22 MAY, 2020
Accepted: 13 JUN, 2020
Available Online: 31 DEC, 2020

Keywords:

Reentry space debris
Low earth orbit
Pulsed laser
Lifetime

ABSTRACT

This research studies the orbital dynamics of space debris in near earth orbit. The orbital dynamics of space debris is closely examined in near earth orbit whereby (apogee altitude ha=1200 km and perigee altitude hp=200 km). In addition, the lifetime of the space debris is calculated using the influence of the friction force exerted on the atmospheric particles with debris dimensions measuring between (1 and 10 cm). In this study, the Drag Thermospheric Models (DTM78 and DTM94) are used because of their dependence on solar and geomagnetic activities, and pulsed lasers are utilized to interact with Aluminum 2024 particles which are frequently employed in the structure of spacecraft and aerospace designs. A numerical analysis program (NaP1) was built to calculate the lifetime of space debris and its time of return to the atmosphere. It is then integrated with a second numerical analysis program (NaP2) developed using the Lax-Wendroff finite difference method to simulate the laser material interaction model. A high power Nd:YAG laser was applied to produce shock wave pressure in target. The results show that the maximum peak pressure occurs at 50 μm depth then slowly decays, the peak pressure increases with the increase of the laser intensity, and the optimum value of the momentum coupling coefficient (Cm) for the aluminum debris of size range (1and10 cm) is 6.5 dyn.s/j.

DOI: http://dx.doi.org/10.31257/2018/JKP/2020/120204

إعادة الحطام الفضائي من المدار الأرضي المنخفض بأستخدام ليزر Nd: YAG النبضي

حامد كريم الزيدي ١ محمد جعفر البيرماني ٢ مهدي طالب رحمة الله ١

١ قسم الفيزياء-كلية العلوم-جامعة بغداد-بغداد- العراق
٢ قسم هندسة تقنيات الحاسوب- جامعة الكفيل- النجف الاشرف-العراق

الكلمات المفتاحية:

اعادة الحطام الفضائي
المدار الفضائي المنخفض
الليزر النبضي

الــخُـلاصــة

في هذا البحث تم دراسة الديناميكيات المدارية للحطام الفضائي في مدار قريب من

الأرض وحساب عمر كل منها. تم فحص الديناميكيات المدارية للحطام الفضائي في مدار قريب من الأرض (ارتفاع الأوج = ١٢٠٠ كم وارتفاع الحضيض = ٢٠٠ كم). بالإضافة إلى ذلك تم حساب عمر الحطام الفضائي بتأثير قوة الاحتكاك على جزيئات الغلاف الجوي بأبعاد الحطام تتراوح بين (١ و ١٠ سم). في هذه الدراسة استخدمت نماذج السحب الحراري (DTM78 و DTM94) وذلك بسبب اعتمادها على الأنشطة الشمسية والمغناطيسية الأرضية ، استخدم في هذه الدراسة الليزر النبضي الأرضي للتفاعل مع جزيئات الألومنيوم ٢٠٢٤ التي تستخدم بشكل واسع في هيكل المركبات الفضائية. تم بناء برنامج تحليل رقمي (NaP1) لحساب عمر الحطام الفضائي وزمن عودته إلى الغلاف الجويودمج مع برنامج التحليل العددي الثاني (NaP2) الذي تم تطويره باستخدام طريقة الاختلاف المحدود Lax-Wendroff لمحاكاة نموذج تفاعل الليزرمع المادة. تم استخدم ليزر Nd: YAG عالي الطاقة لإنتاج ضغط موجة الصدمة على الهدف. أظهرت النتائج أن الحد الأقصى لضغط الذروة يحدث عند عمق ٥٠ ميكرومتر ثم يضمحل ببطء ، ويزداد ضغط الذروة مع زيادة شدة الليزر ، والقيمة المثلى لمعامل اقتران الزخم (Cm) لحطام الألومنيوم في نطاق الحجم (١ و ١٠ سم) هي ٦.٥ داين.ثا|جول.

عمر الحطام

1. INTRODUCTION

Thin-film is called a layer or several layers of material atoms that do not intersect with.

Space debris is defined as man -made objects or parts of in space, which do not serve any useful purpose. In more than 50 years of spaceflight, over 30,000 t of satellites and rockets have been sent to space. It is estimated that near 3000 t of non-functioning space debris remain in [1, 2].

Low Earth Orbit (LEO) in varied forms ranges from fragments to spent rocket bodies and fully intact multi-ton satellite [3]. Since 1957, more than 3500 launches have led to a current population of approximately 9000 tractable objects figure (1) [4, 5]. More than 90% of these objects are space debris. About half of the tractable objects are fragments from explosions or from the backup of satellites or rockets bodies [6, 7]. These debris which are 1 to 10 cm in size are very dangerous because they are difficult to see and yet can punch a big hole in space craft. Larger particles can make punctures to the outer surfaces and may cause damage to structure or equipment by penetration and palliation. Mitigation of debris has been discussed by Metzger, et al. 1989, Phipps 1993, Loftus & Reynolds 1993, Monroe 1994, and Phipps, et al. 1996. Monroe 1994 proposed a ground-based system featuring a 10 m diameter beam director with adaptive optics correction and a 5MW reactor pumped 1.73 µm wavelength laser. Loftus and Reynolds 1993 catalog forces available for removing objects from orbit, including direct propulsion, enhanced aerodynamic drag, solar sail, and electromagnetic drag. A few years ago, a detailed project study were undertaken by Phipps and co-workers to propose a high-energy laser system called ORION.

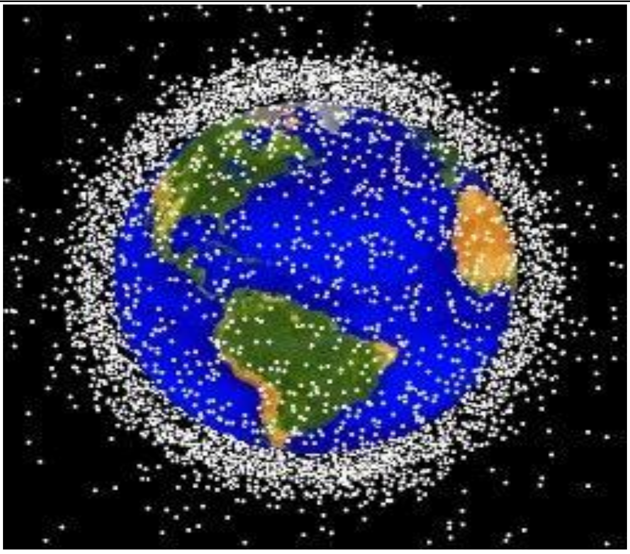

Fig. 1: An impression of the density of occupation the near-earth environment [6,7].

2. Lifetime and Atmospheric Drag Theory

The drag force is given by, $F = \frac{1}{2m} C_D A \rho_a \, v^2$

Where C_D the aerodynamic is drag coefficient, A is the average cross-section area of the debris and ρ_a is the air density. The equations in terms of atmospheric drag are,

$$\frac{dHa}{dE} = \frac{-A}{m} C_D \rho_a \; a(1+e) \frac{(1+e\cos E)^{\frac{1}{2}}}{(1-e\cos E)^{\frac{1}{2}}} (1+\cos E)$$

$$\frac{dHp}{dE} = \frac{-A}{m} C_D \rho_a \; a^2 (1-e) \frac{(1+e\cos E)^{\frac{1}{2}}}{(1-e\cos E)^{\frac{1}{2}}} (1-e\cos E)$$

Runge-Kutta Method was used to solve the above differential equations.

Computer programs are designed to simulate orbit dynamics of space debris lifetime under atmospheric drag force and reentry of space debris under shooting pulsed laser, the atmospheric model adapted is the Drag Thermosphere Model 78,94 (DTM78,94).

3. Laser Material Interaction Theory

The phenomena that occur upon the irradiation of a solid target with a focused high-power laser beam is of interest in the study of laser induced fusion [8, 9]. As a result of the laser irradiation, the plasma (which is produced on the surface) expands mainly in the opposite direction to the oncoming laser beam. A shock wave may penetrate the solid material in the laser beam direction [10, 11].

High power pulsed laser, developed for initial confinement fusion application, and may be used to produce ultrahigh pressures in excess of several mega-bars during a few nanoseconds. The pressure pulse duration is comparable to the laser pulse length [12, 13]. Consequently, the shock decay is externally rapid [14, 15]. The equation that describes shock wave propagation and decay in plane or spherical geometry targets is derived by Harris [14].

$$D\left[(D-u) + \rho C^2 \frac{du}{dP}\right]\frac{DP}{Dx} = \left[(D-u)^2 - C^2\right]\frac{\partial P}{\partial x} - \frac{(n-1)C^2 \rho u (D-u)}{x} \quad (1)$$

where x is the shock front position, $\frac{DP}{Dx}$ is the rate of change of pressure amplitude with distance, n is the geometrical factor (n=1 for plane target and n=3 for spherical target), C is the sound velocity, u is the particle velocity, D is the shock velocity, ρ is the material density and $\frac{\partial P}{\partial x}$ is the gradient of shock pressure immediately behind the shock front. The time dependent version of equation (1) was introduced by Cottet and Romain [13], which is given by.

$$\frac{DP}{Dt} = -A_1 \frac{\partial P}{\partial t} - \frac{A_2}{x + R_0} \quad (2)$$

Where R_0 is the radius of curvature of shock wave at the beginning of decay assumed to be equal to the radius of the laser spot, and the coefficients A_1, A_2 are given by.

$$A_1 = \frac{(D-u)^2 - C^2}{(D-u)D + \rho_0 \frac{D^2 C^2}{(D-u)} \frac{du}{dP} + C^2 - (D-u)^2}$$

$$A_2 = \frac{(n-1)\rho_0 \; DuC^2}{(D-u) + \rho_0 \frac{DC^2}{(D-u)} \frac{du}{dP} + \frac{C^2 - (D-u)^2}{D}}$$

where ρ_0 is the target material density at pressure (P=0). The position of shock front is given by.

$$\frac{Dx}{Dt} = D \qquad (3)$$

The linear relationship between shock wave velocity D and particle velocity u is given by.

$$D = c_0 + Su \qquad (4)$$

where c_0 and S are experimental data [16]. A general expression of sound velocity in target material terms of particle velocity is given by McQueen et al [15].

$$C = \frac{1}{\sqrt{C_0}}[C_0 + u(S-1)]\left[C_0 + 2Su - \frac{\gamma_0 Su^2}{C_0 + Su}\right]^{\frac{1}{2}} \qquad (5)$$

Where C_0 is the sound velocity in the target before the laser irradiation and γ is the specific heat ratio, $\gamma = C_p/C_v$. Pulsed laser impulse coupling to the debris target in the 400-1500 km altitude range is accomplished via the momentum coupling coefficient C_m [17], which is defined as the ratio of target momentum ($m\Delta v$) produced by photo-ablation to incident laser pulse energy W [18, 19].

$$C_m = \frac{m\Delta v}{W} \quad \text{dyne.s/J} \qquad (6)$$

The coupling coefficient has a maximum C_{mopt} because of plasma shielding and other physics. The C_{mopt} normally occurs close to the vapor plasma transition. In this case, we generally cannot predict the nature of the target material, and the targets are certainly not cooperative. As a simplifying factor, all materials of space debris might be composed are likely to have C_{mopt} value in the range 2-10 dyne.s/J.

4. Reentry of Space Debris Theory

In polar coordinates (r,θ) in the fixed plane of two-body orbit problem, including drag force Dg is described by this equation [20,21].

$$\frac{d2r}{dt^2} = \frac{dv_r}{dt} = \frac{v_\theta}{r} - \frac{\mu}{r} - \frac{Dg}{m}\cos\psi \qquad (7)$$

and the angular momentum H is,

$$\frac{d(rv_\theta)}{dt} = -\frac{Dg\ r}{m}\sin\psi$$

which may be combined to give energy,

$$\frac{d\left[\left(v_r^2 + v_\theta^2\right)\left(2 - \frac{\mu}{r}\right)\right]}{dt} = -\frac{Dg\ v\ r}{m}$$

Transforming to θ as the independent variable for convenience, the reentry trajectory is described by the coupled differential equations.

$$\frac{d^2\left(\frac{1}{r}\right)}{d\theta^2} = \frac{\mu}{H^2} - \frac{1}{r} \qquad (8a)$$

$$\frac{dH}{d\theta} = -\rho\, C_D\, \frac{A}{2m} r^2 v \qquad (8b)$$

The first equation remains unchanged from the vacuum case, and the second describes the rate of change of angular momentum, where the drag coefficient $C_D = \frac{2Dg}{\rho\, v^2}$ for hypersonic flight is nearly a constant with the Newtonian value 2. The main idea in this paper is the change of velocity due to laser shooting $r\Delta v$ was added to equation (8) as driving force to de-orbited space debris until the dense atmosphere, the equation becomes,

$$\frac{dH}{d\theta} = -\rho\, C_D\, \frac{A}{2m}\, r^2\, v - r\Delta v \qquad (9)$$

The drag is localized near perigee for an initial highly elliptical orbit, and this essentially produces a negative tangential Δv with no change of perigee, each ensuing orbit having decreased elliptically until a circular condition is reached with nearly the original perigee altitude.

5. Lax-Wendroff Method

Two different methods are used to simulate this study. The first part considers the ablation of aluminum spherical target (space debris) by pulsed laser using a Finite Difference Model (FDM). The second part of this study reentry of this debris from 1200-km altitude to atmospheric region using a Runge-Kutta Method (RKM). This work use the Lax-Wendroff method is adapted for the solution of laser material interaction problem. The derivations of this method can be summarized as follows. Taylor expansion of the function u(x,t) is given by.

$$u(x,t+\Delta t) = u(x,t) + \frac{\partial u}{\partial t}\Delta t + \frac{\partial^2 u}{\partial t^2}\frac{(\Delta t)^2}{2!} + \cdots + O(\Delta t)^2 \qquad (10)$$

This equation can be rendered into index notation form.

$$u_i^{n+1} = u^n + \frac{\partial u}{\partial t}\Delta t + \frac{\partial^2 u}{\partial t^2}\frac{(\Delta t)^2}{2!} + \cdots\cdots + O(\Delta t)^2 \qquad (11)$$

let us consider the wave equation for example,

$$\frac{\partial u}{\partial t} = -\alpha\frac{\partial u}{\partial x} \qquad (12)$$

by differencing the equation (12) in respect to time,

$$\frac{\partial^2 u}{\partial t^2} = -\alpha\frac{\partial}{\partial t}\left(\frac{\partial u}{\partial x}\right) = -\alpha\frac{\partial}{\partial x}\left(\frac{\partial u}{\partial t}\right) = \alpha^2\frac{\partial^2 u}{\partial x^2} \qquad (13)$$

Substituting the above equation in equation (12),

$$u_i^{n+1} = u_i + \left(-\alpha\frac{\partial u}{\partial x}\right)\Delta t + \left(\alpha^2\frac{\partial^2 u}{\partial x^2}\right)\frac{(\Delta t)^2}{2!} \qquad (14)$$

The updated value of the function u at time level n+1 can express in terms of the respective value at time level n as follows:

$$u_i^{n+1} = u_i^n - \alpha\Delta t\left[\frac{u_{i+1}^n - u_{i-1}^n}{2\Delta x}\right] + \frac{\alpha^2(\Delta t)^2}{2}\left[\frac{u_{i+1}^n - 2u_i^n + u_{i-1}^n}{(\Delta x)^2}\right] \qquad (15)$$

The difference scheme of Lax-Wendroff method is then given by.

$$u_i^{n+1} = u_i^n - \frac{c}{2}(u_{i+1}^n - u_{i-1}^n) + \frac{c^2}{2}(u_{i+1}^n - 2u_i^n + u_{i-1}^n) \qquad (16)$$

where $c = \alpha\Delta t$, the scheme given by equation (16) is known as Lax-Wendroff method. A computer program is developed to study the effects of high-power pulsed laser on debris target material. Lax-Wendroff method is used to solve the problem. The normalized scheme of equation (2) is:

$$P_n(i) = P(i) - \frac{t_1\,\Delta t\,D}{2r_o\,\Delta x\,A_1}\frac{1}{2}[P(i+1) - P(i-1)] + \left(\frac{t_1\,\Delta t\,D}{2r_o\,\Delta x\,A_1}\right)^2\frac{1}{2}[P(i-1) - P(i) + P(i+1)] - \frac{t_1\,\Delta t\,Pm\,A_2}{A_1 r_o(1 + x_n(i-1))}$$

The normalization parameters are.

$$P^* = \frac{P}{Pm} \qquad ,t^* = \frac{t}{t_1} \qquad ,x^* = \frac{x}{r_O}$$

6. Results of laser material interaction and Reentry Model

A comparative curve between four values of intensities was obtained by simulation of equation (2) using Lax-Wendroff method of numerical solution. This equation is subject to the boundary values problem. The results are shown in figure (3). The pressure (Mbar) was plotted against target penetration depth (μm). Four values of peak pressure (0.001, 0.005, 0.008, 0.01 Mbar) were resulted from the illumination of aluminum target by pulsed laser of Nd:YAG type (1.06 μm) with pulse duration of 5 ns. The corresponding proposed intensities are (1.5e8, 7.5e8, 1.2e9, 1.5e9 W/cm2) respectively.

The shock wave pressure amplitude increases rapidly after penetration of the target. Maximum pressure occurs at 50 μm depth then decay slow down. It can be seen from this figure that the peak pressure increases with increasing laser intensity. The dynamics of reentry space debris was simulated under the effect of pulsed laser (Nd:YAG type (1.06 μm) shooting near perigee as given by equation (8).

The change of velocity due to laser shooting was added to equation (9) as a driving force to reduce the perigee and apogee altitudes of the debris, until de-orbited in the dense atmosphere. The input parameters are given in tables (1), (2), and (3).

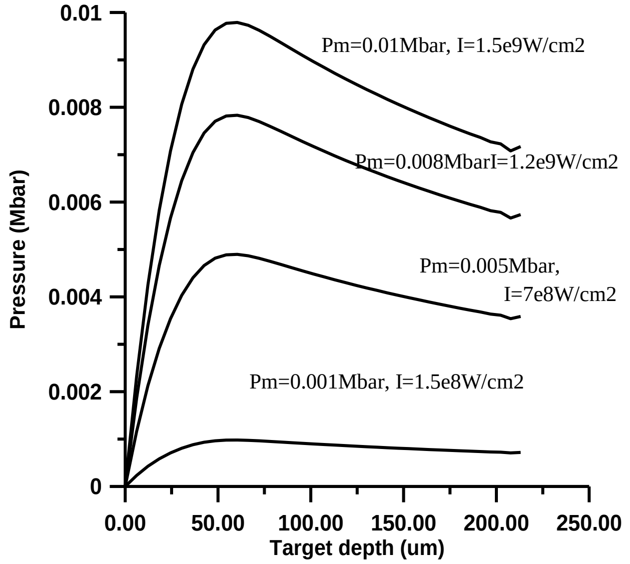

Fig. 2: Shock pressure with target (space debris) depth for laser intensity: 1.5e9, 1.2e9, 7e8, 1.5e8 W/cm^2.

Table 1: Aluminum debris (diameter=10 cm) of reduction in distance (r) of the following orbit parameters.

Energy (J)	336	336	336	336	336
Coupling coefficient Cm (dyn.s/J)	6.5	6.5	6.5	6.5	6.5
dv for each period (m/s)	20	20	20	20	20
Exposition time for each period (min)	16.6*6	16.6*4	16.6*2	16.6*2	16.6*2
Initial Apogee altitude (km)	1200	1000	800	600	400
Initial Perigee altitude (km)	500	500	500	400	200
Final Apogee altitude (km)	1020	672	742	460	260
Final Perigee altitude (km)	500	432	450	285	102
Area/mass (cm^2/gm)	0.0717	0.0717	0.0717	0.0717	0.0717

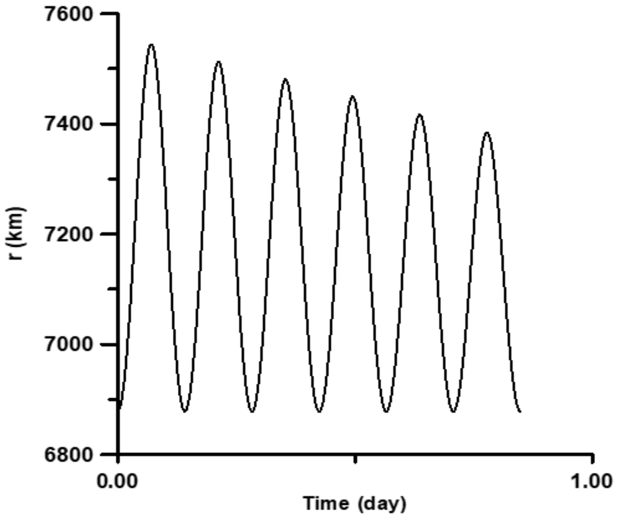

Fig. 3: The time response of geocentric radial distance (r) under pulsed laser irradiation by six shoots of debris (diameter=10cm) with to reentry time from (1200-500km).

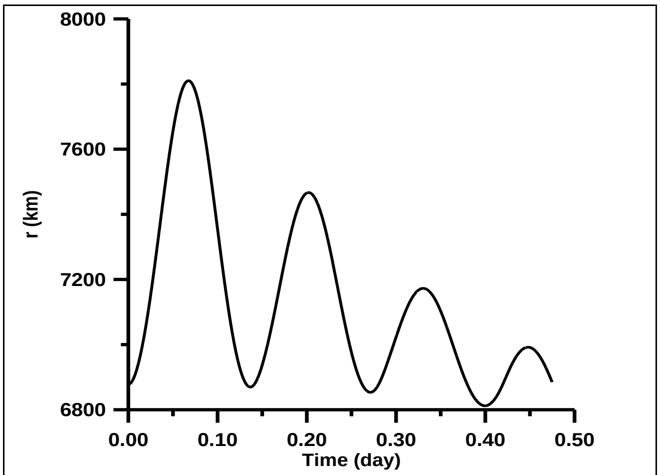

Fig. 4: The behavior of distance of debris (diameter=10cm) with reentry time from (1000-500km) under laser pulsed irradiation (16.66 min each period).

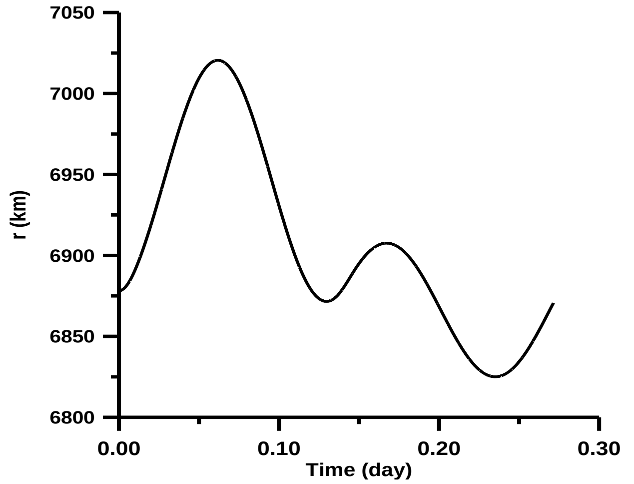

Fig. 5: The behavior of distance of debris (diameter=10cm) with reentry time from (800-500km) under laser pulsed irradiation (16.66 min each period).

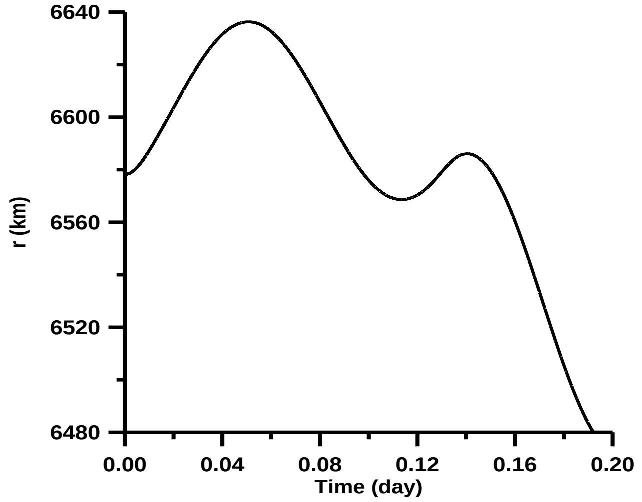

Fig. 6: The behavior of distance of debris(diameter=10cm) with reentry time from (400-200km) under laser pulsed irradiation (16.66 min each period).

The time response of the shooting process for 10 cm debris is shown in figure (3). The radial distance (km) was plotted against reentry time (days). The estimated change in radial distance was (1200-1020 km) at four consecutive pulses, meanwhile the original orbit was (1200-500 km). The same size of debris was shot 4 times at apogee-perigee height (1000-500 km). The result is shown in figure (4). Pulsed laser shooting of the same debris at apogee-perigee altitudes (800-500 km) were applied by two pulses. The result is shown in figure (5). The estimated reduction in apogee-perigee distances was (724-450 km). A quasi circular orbit of space debris of the same size of initial apogee-perigee altitudes (400-200 km) was shot by two pulses (two orbits). The resulted radial distance variation with time is shown in figure (6). The estimated reduction in altitudes was (260-102 km). It was de-orbited to dense atmosphere to burn.

Table 2: Aluminum debris (diameter=1 cm) of reduction in distance (r) of the following orbit parameters.

Energy (J)	336	336	336	336	336
Coupling coefficient C_m (dyn.s/J)	6.5	6.5	6.5	6.5	6.5
dv for each period (m/s)	200	200	200	200	200
Exposition time for each period (min)	6*4	6*4	6*2	6*2	6*2
initial Apogee altitude (km)	1200	1000	800	600	400
initial Perigee altitude (km)	500	500	500	400	200
Final Apogee altitude (km)	510	500	498	400	205
Final Perigee altitude (km)	440	427	430	246	102
Area/mass (cm^2/gm)	0.717	0.717	0.717	0.717	0.717

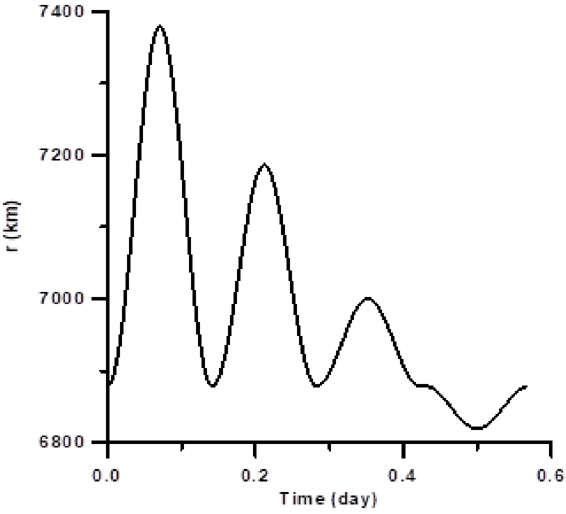

Fig.7: The behavior of distance of debris (diameter=1cm) with reentry time from (1200-500km) under laser pulsed irradiation (6 min each period).

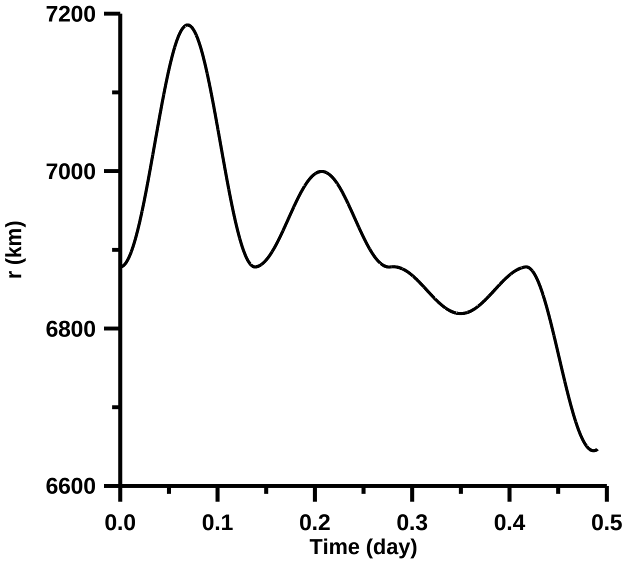

Fig. 8: The behavior of distance of debris (diameter=1cm) with reentry time from (1000-500km) under laser pulsed irradiation (6 min each period).

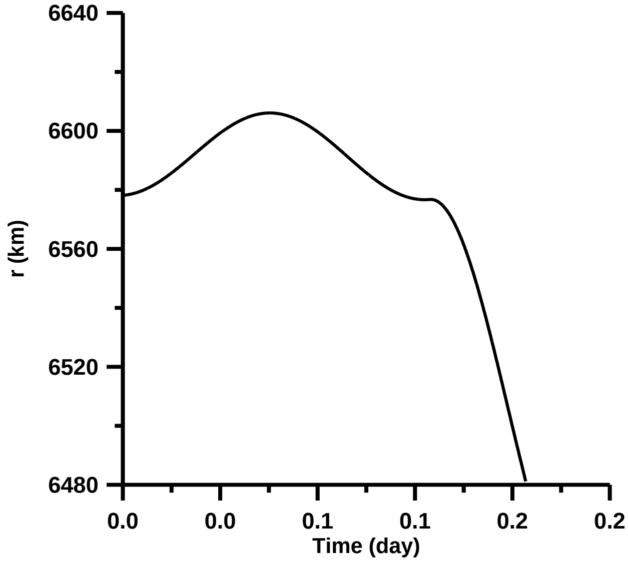

Fig.9: The behavior of distance of debris (diameter=1cm) with reentry time from (400-200km) under laser pulsed irradiation (6 min each period)

The time response of the shooting process for 1 cm debris is shown in figure (7). The radial distance (km) was plotted against reentry time (days). The estimated change in radial distance was (1200-510 km) at four consecutive pulses, meanwhile the original orbit was (1200-500 km). The same size of debris was shot 4 times at apogee-perigee height (1000-500 km). The result is shown in figure (8). It can be seen from this figure that the reduction in apogee and perigee altitude was (500-427 km).A quasi circular orbit of space debris of the same size of initial apogee-perigee altitudes (400-200 km) was shot by two pulses (two orbits). The resulted radial distance variation with time is shown in figure (9), and the estimated reduction in altitudes was (205-102 km). It was de-orbited to dense atmosphere to burn. The reentry time of space debris to different height is depended on many parameters as the following. (a) The laser pulse energy increases the reentry time decreases. (b) The exposition time increases the reentry time decreases. (c)The area to mass ratio A/m increases (in the same conditions) the reentry time decreases. The result of the two pulsed laser shooting of debris 10 cm diameter at apogee-perigee altitudes (1200-500 km) is shown in figure (10).). Sequentially in same parameters to second step (figure 11), the estimated reduction in apogee-perigee altitudes is (155-102 km). By the same process of debris diameter 1 cm, the estimated reduction in apogee-perigee altitudes are (808-499 km), and (152-102 km). The results are shown in figures (12) and (13).

Table 3: Aluminum debris (1, 10 cm) of reduction in distance (r) step by step under the effect of laser pulsed until the space debris de-orbited in atmosphere region of the following parameters.

Energy (J)	336.3 336.3	336.3 336.3	336.3 336.3	336.3 336.3	336.3 336.3
Coupling coefficient Cm (dyn.s/J)	6.5 6.5	6.5 6.5	6.5 6.5	6.5 6.5	6.5 6.5
dv for each period (m/s)	20 200	20 200	20 200	20 200	20 200
Exposition time for each period (min)	16.6*2 6*2	16.6*2 6*2	16.6*2 6*2	16.6*2 6*2	16.6*2 6*2
initial Apogee altitude (km)	1200 1200	865 808	564 499	425 441	241 -
initial Perigee altitude (km)	500 500	488 499	460 441	289 152	122 -
Final Apogee altitude (km)	865 808	564 499	425 441	241 152	155 -
Final Perigee altitude (km)	488 499	460 441	289 152	122 102	102 -
Area/mass (cm^2/gm)	0.0717 0.717	0.0717 0.717	0.0717 0.717	0.0717 0.717	0.0717 0.717

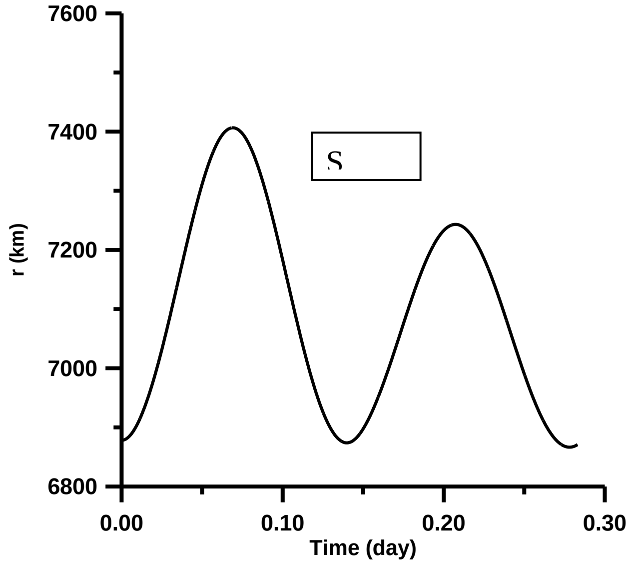

Fig. 10: The radial distance of debris (diameter=10cm) against reentry time from (1200-500km) under pulsed laser irradiation (16.66 min each period).

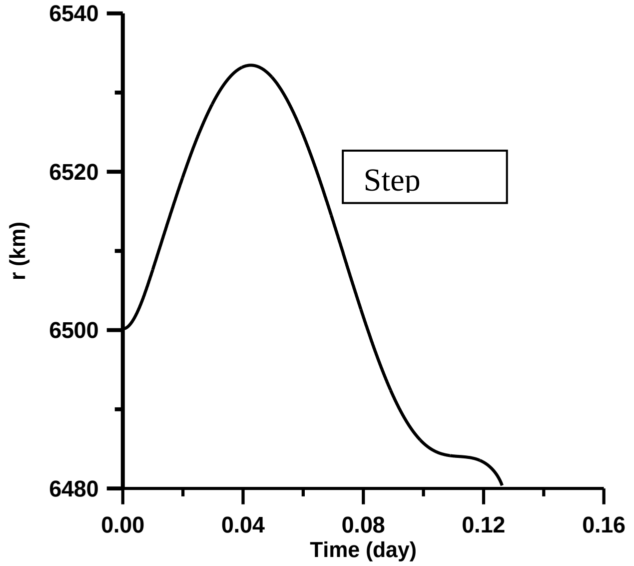

Fig. 11: The radial distance of debris (diameter=10cm) against reentry time from (291-122km) under laser pulsed irradiation (16.66 min each period).

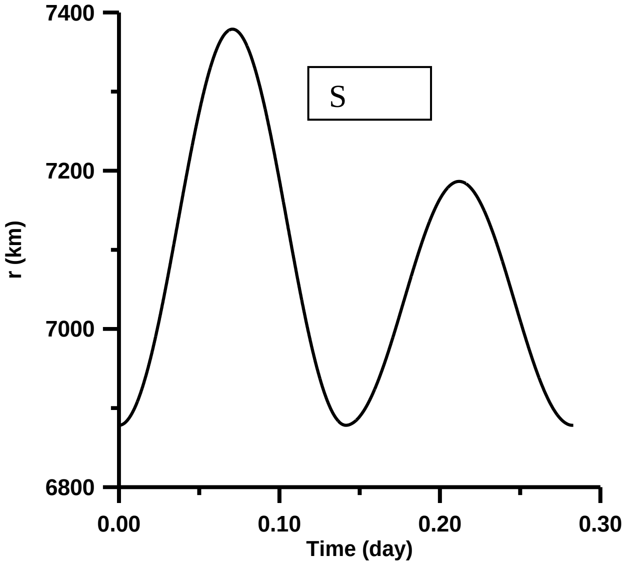

Fig. 12: The radial distance of debris (diameter=1cm) against reentry time from (1200-500km) under laser pulsed irradiation (6 min each period).

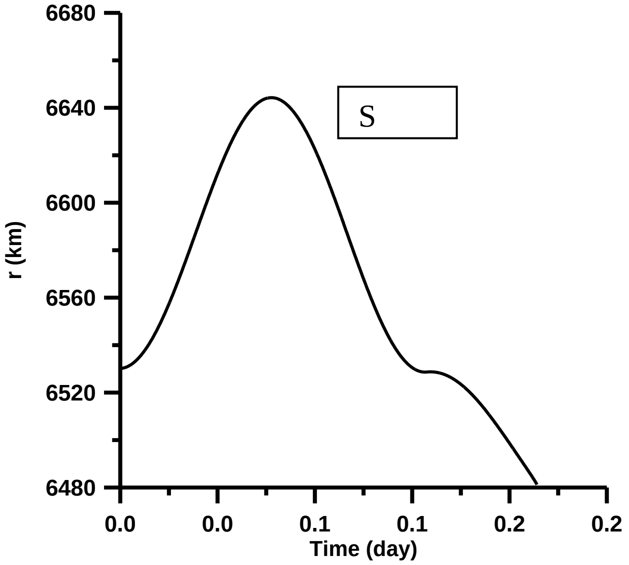

Fig. 13: The radial distance of debris (diameter=1cm) against reentry time from (441-152km) under laser pulsed irradiation (6 min each period).

Aluminum debris (diameter = 10, 1 cm) of change the d(1/r)/d(theta) respect to distance (r) of the same parameters of orbit parameters are shown in tables (2) and (3). The clearance of the outer space (low earth orbit from space debris) can be performed by shooting the targets by laser beam. The resulted change in orbital velocity Δv at perigee would transfer the elliptical orbit gradually into near earth circular orbit. This process is shown in figure (14). This is the state space plot of against. The selected target material was aluminum 2024 of size 10 cm at initial apogee-perigee altitudes 1200 and 500 km respectively. The target was shot for six orbits of time duration 16.6 minute per orbit at perigee. It can be seen from this figure that the shape and size of the orbit is gradually changed from elliptic to circular. As a result of these, shooting the apogee altitude would decrease from 1200 km to 1020 km at constant perigee altitude. Figure (15) shows the state space plot of against for a space debris of size 1 cm the initial orbit was apogee=1200 km and perigee = 500 km. The space debris was shot four times of 6 minutes per orbit. The resulted final orbit was apogee=510 km and perigee=440 km.

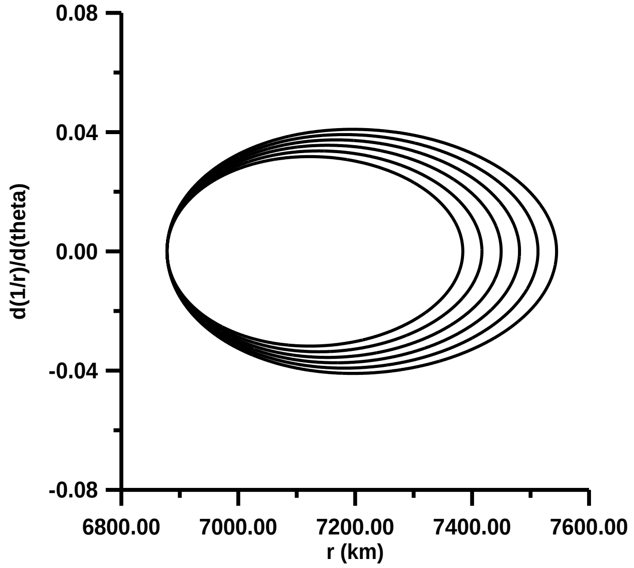

Fig. 14: The reentry trajectory from (altitude=1200-500km) under laser pulsed irradiation (16.6 min each period).

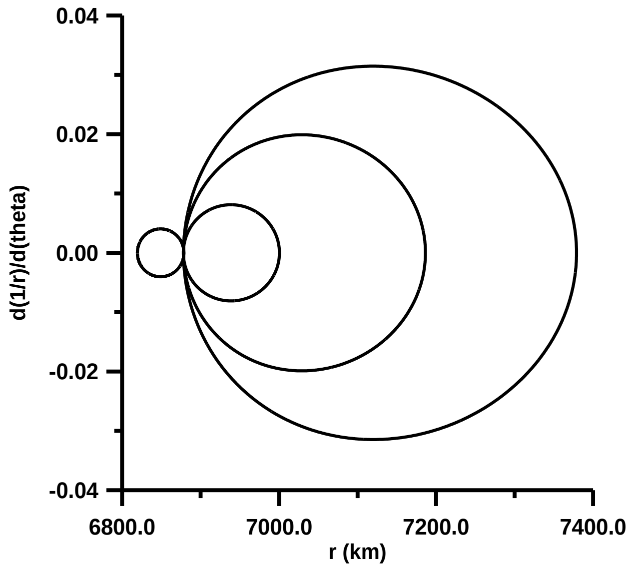

Fig. 15: The reentry trajectory (diameter=1cm) from (1200-500km) under laser pulsed irradiation (6 min each period).

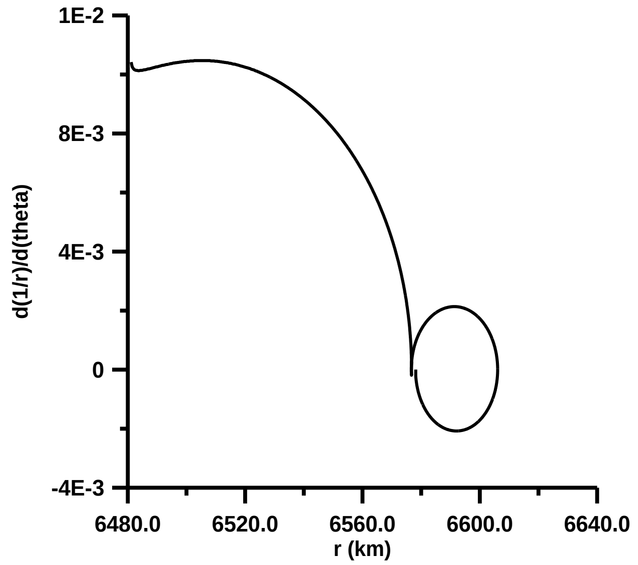

Fig. 17: The reentry trajectory (diameter=1cm) from (400-200km) under laser pulsed irradiation (6 min each period).

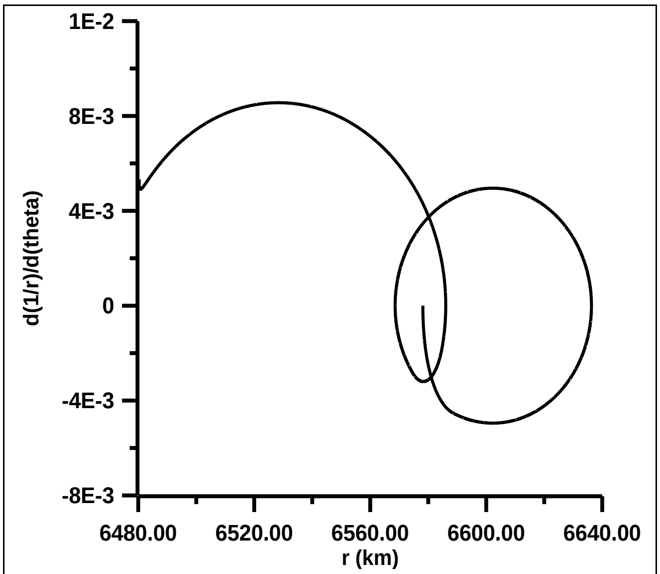

Fig. 16: The reentry trajectory (diameter=10cm) from (400-200km) under laser pulsed irradiation (16.66 min each period.

Figure (16) shows the change of the debris orbit due to laser shooting two times of duration 16.6 minutes per orbit. The initial orbit altitudes were apogee=400 km and perigee=200 km. The final orbit dimensions were apogee=260 km and perigee=102 km. Figure (17) shows the change of the debris orbit due to laser shooting two times of duration 16.6 minutes per orbit. The initial orbit altitudes were apogee=400 km and perigee=200 km. The final orbit dimensions were apogee=205 km and perigee=102 kmFig. 18 the reentry trajectory (diameter=10cm) from (400-200km) under laser pulsed irradiation (16.66 min each period).

3. CONCLUSIONS

Reentry dynamics of orbital debris have been modeled and solved numerically. It has been found that shock wave formation by irradiation of clusters of space debris by high power pulsed laser depends on the fluence and pulse duration. An impulse imparted to the debris might cause a change in orbital velocity Δv. This increment of orbital velocity will reduce the ellipticity of the orbital motion gradually into near earth circular, then deorbited in the dense atmosphere. For the 10 cm debris that the estimated change in radial distance was (1200-1020 km) at four consecutive pulses, meanwhile the original orbit was (1200-500 km). The same size of debris was shot 4 times at apogee-perigee height (1000-500 km). Pulsed laser shooting of the same debris at apogee-perigee altitudes (800-500 km) were applied by two pulses. The estimated reduction in apogee-perigee distances was (724-450 km). A quasi circular orbit of space debris of the same size of initial apogee-perigee altitudes (400-200 km) was shot by two pulses (two orbits). The estimated reduction in altitudes was (260-102 km). It was de-orbited to dense atmosphere to burn. While for 1 cm debris the estimated change in radial distance was (1200-510 km) at four consecutive pulses, meanwhile the original orbit was (1200-500 km). The same size of debris was shot 4 times at apogee-perigee height (1000-500 km and the reduction in apogee and perigee altitude was (500-427 km).A quasi circular orbit of space debris of the same size of initial apogee-perigee altitudes (400-200 km) was shot by two pulses (two orbits), and the estimated reduction in altitudes was (205-102 km). It was de-orbited to dense atmosphere to burn. The mechanical coupling coefficient (Cm) was verified theoretically and the optimum value for aluminum debris of size range (1and 10 cm) was Cm =6.5 dyn.s/J. Results of simulation show that reentry time can be controlled according to variables of the number of shooting per orbit at perigee, pulse duration, laser spot size, target material density, and laser intensity.

4. REFERENCES

[1] Phipps C. R., Baker K. L., Libby S. B., Liedahl D. A., Olivier S. S., Pleasance L.D., Rubenchik A., Trebes J. E., George E. V., Marcovici B., Reilly J. P., and Valley M. T., “Removing Orbital Debris with Pulsed Lasers”, Advances in Space Research, vol. 49, 2012, pp. 1283-1300.

[2] Liou J. C., and. Krisko P. H.,” An update on the effectiveness of Postmission disposal in LEO”, Proceedings of the 64th International Astronautical Congress, IAC-13-A6.4.2, Beijing, China, 2013.

[3] Ebisuzaki T., Quinn M. N., Wada S., L. Piotrowski W., Takizawa Y., Casolino M., Bertainac,d M. E., Gorodetzky P., Parizot E., Tajima T., Soulardb R., and Mourou G., “Demonstration designs for the remediation of space debris from the International Space Station”, Acta Astronautica, vol. 112, 2015, pp. 102–113.

[4] Shuangyan S., Xing J., and Hao Ch., “Cleaning space debris with a space-based laser system”. Ch. J. of Aeronautics, vol. 27, Issue 4, 2014, pp. 805–811.

[5] Hampf D, Riede W., Stockle G., and Buske I., “Ground-Based Optical Position Measurements of Spac Debris in Low-Earth Orbits”,DeutscherL Raumfahrtkongres ((Institute of Technical Physics, Germany)), 2013, Document ID: 301313.

[6] Eichler P., and Rex D., "Collision risk in space-detailed analysis and basic consequences for design and operation of larger structure", The International Symposium of Space Dynamics took place, Toulouse, France, Nov. 1989.

[7] Walker R., Sdunnus H., and Klinkrad H., "Update of the EAS Space Debris Mitigation Handbook", Qinetiq/KI/Space/CR021539, 2002.

[8] Arad B., Elieze S., Gazit Y., Loebenstein H. M., Zigler A., Zmora

H., and Zweigenbaum S., "Burn-through of thin aluminum foils by laser-driven ablation", J. Appl. Phys. Vol. 50, Issue 11, 1979, pp. 6817-6821.

[9] Remingtion B. A, Bazan G., Belak J., Bringa E., Caturla M., Colvin J. D., and Edwards M. J., "Materials science under extreme conditions of pressure and strain rate", Metallurgical and Materials Transactions A, vol. 35A, Issue 9, 2004, Article 2587. 20

[10] Clark T.R, and Milchberg H. M., "Optical mode structure of the plasma waveguide", Phys Rev E, vol. 61, no. 2, 2000, pp. 1954-65.

[11] Zhigilei L. V., and Dongare A. M., "Multi-scale modeling of laser ablation: Application to nanotechnology", CMES, vol. 3, no. 5, 2002, pp. 539-555.

[12] Harilal S. S, Bindhu C. V., and Kunze H. J., "Space and time resolved soft x-ray emission from laser produced magnesium plasma", Appl. Phys., vol. 34, no. 4, 2001, pp. 560-566.

[13] Fang Y., Yang L., Zhao Sh., Wang Y." Numerical simulation and experiments of ground-based laser irradiating small scale space debris", Optik, vol. 127, no. 3, 2016, pp. 1078-1083.

[14] Cottet F., and Romain J. P., "Formation and decay of laser generated shock wave", Phys Rev A, vol. 25, no. 1, 1982, pp. 576-579.

[15] Taleb A. M., and Abdulla M. M., "Generation and Decay of Laser Driven Shock Waves", Fondazione Giorgio Ronchi, Anno LVIII, no.1, 2003, pp.71-77.

[16] McQueen R. G., Marsh S. P., Taylor J. W., Fritz J. N., and Carter W. J., " The Equation of State of Solids from Shock Wave Studies ", High Velocity Impact Phenomena, Edited by R. Kinslow, New York, 1970, Chap. VII, pp. 293-417.

[17] Scharring S., Wilken J., and Eckel H., "Laser-based removal of irregularly shaped space debris", Optical Engineering, vol. 56, no. 1, 2017, 011007(1-9).

[18] Early J. T., Bibeau C., and Phipps C. R., "Space debris de-orbiting by vaporization impulse using short pulse laser", AIP Conference Proceedings, vol. 702, no. 190, Sendai (JAPAN), 2004.

[19] Phipps C.R., "Advantages of using picosecond pulses in the ORION space debris clearing system", Proc. International Conference, Lasers and applications, New Orleans, 1998, pp. 935-941.

[20] Campbell J.W., "Project ORION: Orbital debris removal using ground-based sensors and laser", Marshall Space Flight Center, Alabama, NASA Technical Memorandum 108522, 1996.

[21] Geyling F. T., and Westerman H. R., "Introduction to Orbital mechanics", Addison-Wesley Publishing Company, USA, 1971.

[22] Z. Petrovid, and S. Stupar, "Computational Fluid Dynamics one", Mechanical Engineering Faculty, Belgrade, 1996.

[23] J. D. Andorson "Computational Fluid Dynamics ", McGraw-Hill Series, New York, 1995.